# RADIAL VELOCITY AMBIGUITY RESOLUTION FOR THE PULSED SPACE SURVEILLANCE RADAR GESTRA

**Simon Kollecker and Steven Horstmann**

*Fraunhofer FHR, Fraunhofer Institute for High Frequency Physics and Radar Techniques FHR, Wachtberg, Germany.*
*Email: {simon.kollecker, steven.horstmann}@fhr.fraunhofer.de*

## ABSTRACT

Pulsed radars, such as the German Experimental Space Surveillance and Tracking Radar (GESTRA), can be a helpful tool for the improvement of Space Situational Awareness (SSA) required for sustainability and safety of satellite missions. However, their Doppler estimation may loose accuracy due to an ambiguity equal to the Pulse Repetition Frequency (PRF). In this study, we analyze three algorithms that resolve this ambiguity through tracking, two of which are novel, while the third one already exists in literature. One method only propagates the radial motion, while the others perform Initial Orbit Determination (IOD). We evaluate the algorithms' performance – and their ability to self-assess correctness of the result – using real experiments from GESTRA as benchmarks. A method using a Gaussian Sum Filter (GSF) for IOD gives the correct results in almost all examples. The use of such algorithms can significantly enhance the estimation accuracy for radar systems such as GESTRA.

Keywords: Doppler; Ambiguity; SSA; Space Surveillance; Radar; GESTRA; Space Debris.

## 1. INTRODUCTION

Many parts of modern infrastructure and research depend on space flight and satellites. However, the increasing number of satellites and debris objects also increases the probability of collisions. Due to high orbit velocities, a collision is typically fatal when the impacting object is larger than $1\,\mathrm{cm}$, creating a new debris cloud. If no active action is performed to prevent collisions, this could result in a chain reaction called Kessler syndrome [5], which could potentially render e.g. the Low Earth Orbit (LEO) too dangerous for further space missions [8]. Maintaining a catalog of space objects is a first step to prevent this risk as it allows for evasion maneuvers of operational satellites.

Apart from telescopes and lasers, radars are employed to track space objects, as they operate independent of local weather and daylight conditions. However, radars operating on ranges as high as the distance from earth to a satellite require a high amount of energy. Hence, in monostatic configuration, the receiver is likely to be saturated by the transmitter. This motivates the use of pulsed radars, i.e. radars that transmit energy for a short time and then wait for the echo before transmitting again.

Depending on the radar system, different estimation parameters can be affected by ambiguities. While coherent radar networks can have a Direction-of-Arrival (DoA) ambiguity [10], it is well known that a single pulsed radar can already have an ambiguity in range and/or Doppler. This typically depends on the Pulse Repetition Frequency (PRF): while a high PRF produces range ambiguities, a low PRF typically gives rise to Doppler ambiguities [12, Chapter 4]. Depending on the radar frequency and the scenery, it may not be possible to avoid both of them. However, such ambiguities can be resolved by several techniques, of which there are mainly two categories: Methods in the tracking stage and modifications in the system design. For the latter, a prominent example is a variable or staggered PRF [13, 14]. In many cases, this is not desired, because it requires adaptation of many components of a radar system; these adaptations usually need a significant amount of work. Hence, from a practical point of view it is often easier to resolve ambiguities a posteriori at tracking stage. There, the exact algorithm usually depends on the application, because it is necessary to have some knowledge about the target motion. The case for constant velocity in 2D is treated in [11]. In space surveillance, one can search for the most likely Kepler orbit for a set of given detections, assuming a suitable noise model [18]. For this optimization, [18] leaves out the Doppler information because of its ambiguity. However, it is also possible to treat the noise probability distribution in Doppler as a weighted sum of shifted Gaussians [19]. One of the novelties of this paper is the application of such a Gaussian Sum (GS) for Doppler ambiguity resolution in the space surveillance domain utilizing Initial Orbit Determination (IOD) and the full detection information. Another novelty is the introduction of the Radial Velocity Propagation (RVP) as an alternative ambiguity resolution method.

These methods are compared in the context of the German Experimental Space Surveillance and Tracking

*Proc. 9th European Conference on Space Debris, Bonn, Germany, 1–4 April 2025, published by the ESA Space Debris Office*
*Editors: S. Lemmens, T. Flohrer & F. Schmitz, (http://conference.sdo.esoc.esa.int, April 2025)*

Radar (GESTRA) [17, 16, 6, 7], which observes the LEO using search and tracking modes. As we will see in the next section, it is affected by a Doppler ambiguity.

The paper is organized as follows. Section 2 presents the Doppler ambiguity challenge specifically in the context of GESTRA. Section 3 introduces two new Doppler ambiguity resolution methods using radial acceleration, as well outlining the method from [18]. Section 4 tests all of these methods on several selected experiments performed by GESTRA. Section 5 concludes the results and gives an outlook of possible future work.

## 2. SCENARIO

In this section, we will give an overview over GESTRA and the problem of Doppler ambiguities in this context.

### 2.1. GESTRA working principle

GESTRA [17] is a quasi-monostatic pulsed phased array radar featuring a separate transmitter and receiver located approximately $100\,\mathrm{m}$ apart. Its primary objective is the detection and tracking of objects in LEO. The system offers several search modes, as well as a tracking mode. Each search mode continuously monitors a specific volume in space, known as the Field of View (FoV), which consists of multiple beam positions. GESTRA employs electronic beam steering to periodically cycle through them. The duration of a complete scan cycle, or revisit time, is less than approximately $5.5\,\mathrm{s}$. In tracking mode, the operator inputs a Two Line Element (TLE) dataset describing an orbit, allowing GESTRA to follow the object along its propagated trajectory as long as it remains within an angle accessible to electronic beamsteering. This results in a higher number of detections for this particular object with shorter temporal intervals between them. In each instance, GESTRA transmits multiple consecutive pulses in the same direction, which are then integrated to form a Coherent Processing Interval (CPI).

### 2.2. The Doppler ambiguity issue

In this paper, range $\rho$, radial velocity $\dot{\rho}$ and radial acceleration $\ddot{\rho}$ will refer to the round-trip ranges (the full distance transmitter-object-receiver) and its derivatives. It is well known that standard pulsed radars have a range ambiguity of $\rho_{amb} = c_0/f_{pr}$ and a radial velocity ambiguity of $v_{amb} = f_{pr} c_0 / f_0$, where $c_0$ denotes the speed of light. Typical values for GESTRA are shown in Table 1. The PRF is chosen low enough to prevent range ambiguity. However, such a low PRF results in a very severe Doppler ambiguity: Since the round-trip radial velocities in this scenario can easily reach $\pm 14\,\mathrm{km/s}$, standard radar theory would suggest the existence of thousands of candidates for the correct radial velocity. However, the long pulses require compensation of Doppler frequency even within a single pulse, not only across pulses. Hence, for every radial velocity under test, the reference function is Doppler-transformed, before the correlation is computed. While within a single pulse, a compensation for Doppler (i.e. radial velocity) is required, the interpulse phase correction even requires compensation for radial acceleration. This allows estimation of the radial acceleration, which is unambiguous by design.

*Table 1. Parameters of GESTRA in this study.*

| symb. | parameter name | approx. value |
|---|---|---|
| $f_0$ | Transmit frequency | L band |
| $B$ | Bandwidth | $2\,\mathrm{MHz}$ |
| $d$ | dutycycle | $16\,\%$ |
| $T_p$ | pulse length | $2, 4.5\,\mathrm{ms}$ |
| $f_{pr}$ | PRF | $83, 37\,\mathrm{Hz}$ |
| $v_{amb}$ | rad. vel. ambiguity | $19, 8.5, 6\,\mathrm{m/s}$ |
| $N_p$ | no. of pulses to integrate | $3 - 40$ |
| $T_{CPI}$ | CPI length: $f_{pr} \cdot N_p$ | $0.2 - 0.8$s |

As a result, the single-pulse Doppler compensation provides an unambiguous but inaccurate Doppler estimate, while the estimate due to compensation across pulses is accurate but ambiguous. An overall accurate estimate would require the single pulse accuracy to be sufficient to resolve the interpulse ambiguities. Since the ambiguity in Doppler is equal to the PRF and the accuracy of the single pulse estimate scales with the pulse length $T_p$, this depends on the dutycycle $f_{pr} \cdot T_p$. Figure 1 shows the noise-free ambiguity function for this case. We see that the sidelobes at the first ambiguity are closer than $0.5\,\mathrm{dB}$ to the maximum. This means that even low noise levels might be able to push the sidelobe over the maximum, which would result in a radial velocity error of one ambiguity. Figure 2 shows the consequence of it: The plot depicts the error in radial velocity of a tracking mode experiment performed with the Sentinel-3A satellite, compared to accurate orbit data [2]. We see that the error is always close to the multiple of some number, which is the ambiguity caused by the chosen PRF.

There is one immediate strategy to improve the performance and increase the number of detections at the correct ambiguity: A refinement in the radial velocity grid. For the sake of a small computing time, the grid in all search directions is initially set up in a way such that the grid value closest to the true maximum gives a power that is closer than $3\,\mathrm{dB}$ to the maximum. We found that the sidelobes amplitude can be much closer than that to the real maximum. Whenever the first sidelobe is closer to a grid point than the true maximum, the detector may choose this sidelobe over the true maximum even at high Signal to Noise Ratio (SNR). Hence, it makes sense to employ a finer radial velocity grid in order to reduce ambiguity-induced errors. In order to prevent a significant increase in processing time, this refinement is performed a posteriori for each detection in a small radial velocity environment. A comparison of the two plots of Figure 2 shows a significant improvement even though

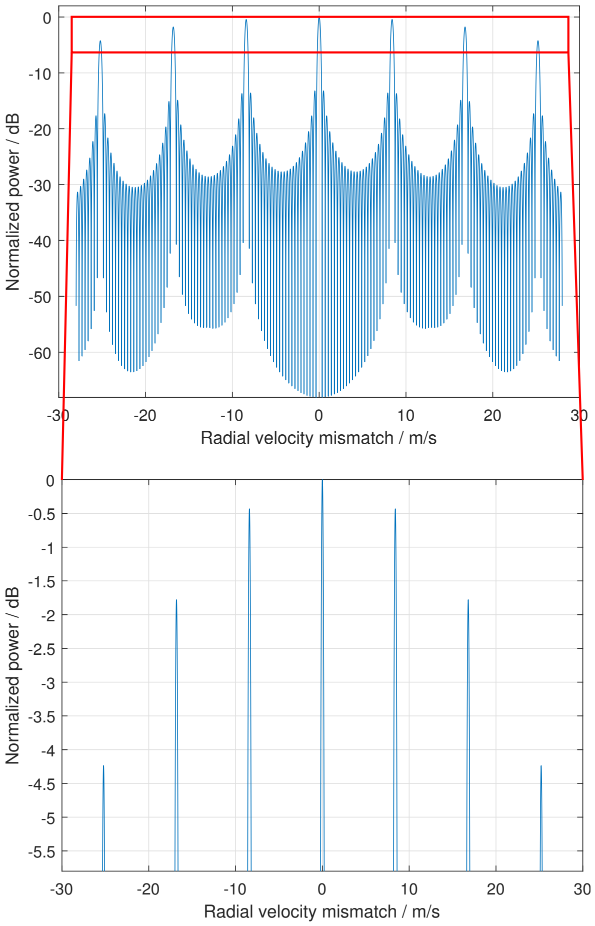


*Figure 1. Ambiguity function in radial velocity: Correlation result for an artificial target without noise around the correct radial velocity of zero; the maximum is scaled to* 0 dB*. The top plot shows the full function, the bottom plot zooms into the upper part of the y axis. Scenario:* 24 *pulses,* $f_{pr} = 37\,\mathrm{Hz}$*,* $T_p = 4.5\,\mathrm{ms}$.

the ambiguity effect is still clearly visible in case of a refined radial velocity grid.

Moreover, these plots illustrate that a resolution of the ambiguity could significantly reduce the radial velocity error. The algorithms presented here shall change each radial velocity of a tracklet by a multiple of $v_{amb}$, such that we ideally always get the correct ambiguity. They shall not use any external knowledge of the satellite's orbit.

The radial parameters estimated by GESTRA are range $\rho$, ambiguous radial velocity $\dot{\rho}_a$ and range acceleration $\ddot{\rho}$. As seen before, ambiguous radial velocity means that the value might differ from the true value by a small integer times $v_{amb,k}$. There is also an estimation of the DoA parameters $u$ and $v$, which parametrize the components tangential to the antenna plate of the normalized vector from the antenna to the target. The DoA estimation is performed using multiple receive channels steered in different directions and their differences in measured phase

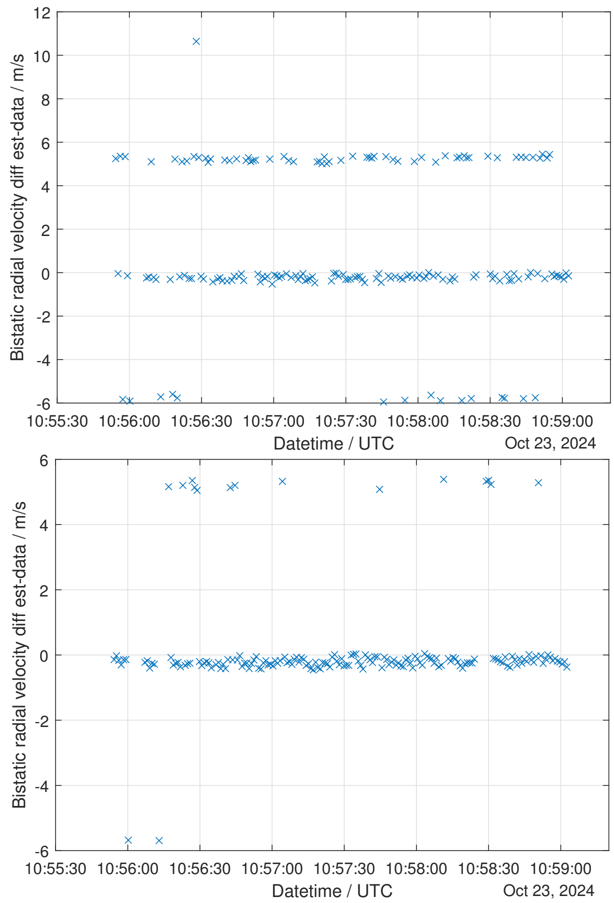


*Figure 2. Error in radial velocity for a tracking mode experiment with the Sentinel 3A satellite. Top: without refinement of the radial velocity grid. Bottom: with* 10*x refinement of the velocity grid.*

and amplitude. The standard deviation of the observed parameters is estimated as well, which will be denoted by $\sigma_\rho$, $\sigma_{\ddot{\rho}}$, $\sigma_u$, $\sigma_v$ and $\sigma_{\dot{\rho},una}$, where $\sigma_{\dot{\rho},una}$ means the standard deviation of the unambiguous radial velocity, i.e. the standard deviation we would have if we could resolve all ambiguities perfectly.

Hence let us assume that we have a tracklet of $N$ detections, i.e. for $k = 1, \ldots, N$, we are given $t_k$ (i.e. the time of the detection), $\rho_k$, $\dot{\rho}_{a,k}$, $\ddot{\rho}_k$, $u_k$, $v_k$, $\sigma_{\rho,k}$, $\sigma_{\dot{\rho},una,k}$, $\sigma_{\ddot{\rho},k}$, $\sigma_{u,k}$ and $\sigma_{v,k}$. This is the input data for the algorithms presented in the next section.

## 3. AMBIGUITY RESOLUTION METHODS

In this section, we will present three methods: It will start with the Radial Velocity Propagation (RVP) method that is easy to implement, because it does not require any orbit determination but uses basic quadratic equations of motion. Next, we will shortly present a method introduced in [18] based on Initial Orbit Determination (IOD) and Weighted Least Squares (WLS). Finally, we will present an original method using a Gaussian Sum Filter (GSF) for the IOD.

### 3.1. Radial Velocity Propagation (RVP)

This approach uses the assumption that on small time scales between detections, the radial motion of an object in LEO is approximately quadratic. Since GESTRA measures radial acceleration, this allows the prediction of the next radial velocity from the previous one.

The algorithm is constructed as follows. We assume that the true radial velocity value of the first detection lies within an interval of $b \in \{-3, \dots, 3\}$ ambiguities. While we have seen a distance of at most two ambiguities in these experiments, this leaves some room for outliers. Hence, the corrected first radial velocity value, dependent on $b$, is

$$\dot{\rho}_{b,1} := \dot{\rho}_{a,1} + b v_{amb}. \tag{1}$$

Now, for each of these start hypotheses, we try to resolve the whole tracklet, one detection at a time: Consider $\dot{\rho}_{b,k-1}$, then let

$$\dot{\varrho}_{b,k} := \dot{\rho}_{b,k-1} + (t_k - t_{k-1}) \cdot \frac{1}{2}(\ddot{\rho}_{k-1} + \ddot{\rho}_k) \tag{2}$$

be the reference radial velocity, propagated from the previous one and the observed radial accelerations. Then, define the resolved ambiguity by

$$\dot{\rho}_{b,k} = \underset{v \in \dot{\rho}_{a,k} + v_{amb}\mathbb{Z}}{\arg\min} |\dot{\varrho}_{b,k} - v| \tag{3}$$

as the ambiguity that is closest to the reference radial velocity. Completing this for the whole tracklet results in one corrected tracklet for each value of $b$, among which we have to choose. For this choice, we exploit that on average over the signed velocity error, we are closer to the correct ambiguity than to any other ambiguity. Hence, we define the average correction to be

$$S_b := \frac{1}{N} \sum_{k=1}^{N} (\dot{\rho}_{b,k} - \dot{\rho}_{a,k}). \tag{4}$$

Then, we choose the value of $b$ that minimizes $|S_b|$. Note that the average is taken over the signed differences, meaning that if the upper and lower ambiguity is chosen equally often, $S_b$ will be close to zero.

The method relies on two crucial assumptions, which might lead to failures in case they are not fulfilled. On the one hand, it assumes that the motion from one detection to the next is approximately quadratic. If the variation of the radial acceleration is high enough, such that it causes the argmin in (3) not to choose the correct value, the method will fail in the sense that either the detection before or the detection after can be resolved correctly, but not both. This problem may arise whenever the temporal distance between two consecutive detections becomes too high. In this case, most likely some corrected radial velocities in the resulting tracklet will be correct, while others will be wrong. The other assumption is that the choice of minimizing $|S_b|$ actually gives the correct ambiguity. This may break if the distribution of ambiguities is strongly biased, e.g. if more detections are one ambiguity above than in the correct one. It is most likely to happen, when we have a small number of detections, because then it is statistically more likely. In that case, all results are wrong.

The minimum value in (3) is an indication for the resolution success: By definition, this is less than $\frac{1}{2}v_{amb}$, so dividing it by $\frac{1}{2}v_{amb}$ gives a number between 0 and 1. The maximum of this value over the whole experiment for the chosen value of $b$ will be called uncertainty. When this is always close to zero, the choice for the ambiguity was very clear. When it is close to 1, there were cases in which almost another ambiguity would have been chosen. As well as the uncertainty for this choice, we can define the uncertainty for the choice of $b$: When dividing the minimum $|S_b|$ by the second smallest $|S_b|$ value, we get a number between 0 and 1 that is close to 0 when the minimum was very clear and close to 1 if it was unclear. In the end, the total uncertainty is chosen as the maximum of all the individual uncertainties.

### 3.2. Herrick-Gibbs and iterative nonlinear Weighted Least Squares (WLS)

The method from [18] is based on IOD with a refinement step using an iterative nonlinear WLS algorithm. As input the DoA as well as the range estimation is used. The required steps are [18]

1. Calculate initial state $x_0$ using Herrick-Gibbs IOD
2. Propagate $x_0$ to all observation times and get the Jacobian matrix $H$
3. Iterative WLS: $\Delta x_{0,lsq} = \left(H^T W H\right)^{-1} H^T W \Delta z$, with the weighting matrix $W$ calculated using the measurement noise variances
4. Repeat steps 2 and 3 until convergence
5. Propagate the orbit to get the radial velocity and correct the radial velocity measurements

The Herrick-Gibbs IOD algorithm is described in [15], utilizing their provided code.

### 3.3. Initial Orbit Determination using Gaussian Sum Filter (GSF)

Similarly to the previous one, this method uses IOD. In contrast to the previous one, it does not only use DoA and range but the full information of the detection. Instead of an iterative nonlinear WLS algorithm this method uses a Particle Swarm Optimization

(PSO) approach to determine the orbit $\theta$. The parameter $\mathbf{y}_{k,1:4} = [u_k, v_k, \rho_k, \ddot{\rho}_k]$ with its covariance $R_{k,1:4} = \operatorname{diag}\left(\left[\sigma^2_{u,k}, \sigma^2_{v,k}, \sigma^2_{\rho,k}, \sigma^2_{\ddot{\rho},k}\right]\right)$ are given by the tracklet and are assumed to follow a multivariate normal distribution

$$f_{\mathcal{N}_4}\left(\mathbf{y}_{k,1:4} \mid \mathbf{y}^-_{k,1:4}, R_{k,1:4}\right) = \frac{1}{(2\pi)^2\sqrt{|R_{k,1:4}|}} \cdot \\ \exp\left(-\frac{1}{2}\left(\mathbf{y}_{k,1:4} - \mathbf{y}^-_{k,1:4}\right)^\top R^{-1}_{k,1:4}\left(\mathbf{y}_{k,1:4} - \mathbf{y}^-_{k,1:4}\right)\right), \tag{5}$$

where $\mathbf{y}^-_{k,1:4}$ is the propagated and transformed orbit at time $k$. The ambiguous radial velocity is modeled as weighted GS with $J$ components such that

$$\sum_{j=1}^{J} w_j f_{\mathcal{N}}\left(y_{k,5} \mid y^-_{k,j,5}, R_{k,5}\right) = \\ \sum_{j=1}^{J} w_j \frac{1}{\sqrt{2\pi R_{k,5}}} \exp\left(-\frac{(y_{k,5} - y^-_{k,j,5})^2}{2R_{k,5}}\right), \tag{6}$$

with the GS weights

$$\sum_{j=1}^{J} w_j = 1, \quad \text{with} \quad w_j \geq 0, \tag{7}$$

using the measured radial velocity $y_{k,5} = \dot{\rho}_{a,k}$ and the unambiguous variance $R_{k,5} = \sigma^2_{\dot{\rho},una,k}$. The propagated and shifted radial velocity is denoted by $y^-_{k,j,5}$. The combined total likelihood of $N$ measurements is

$$L(\theta; \{\mathbf{y}^{(k)}\}^N_{k=1}) = \prod_{k=1}^{N}\left[f_{\mathcal{N}_4}\left(\mathbf{y}_{k,1:4} \mid \mathbf{y}^-_{k,1:4}, R_{k,1:4}\right) \cdot \\ \left(\sum_{j=1}^{J} w_j f_{\mathcal{N}}\left(y_{k,5} \mid y^-_{k,j,5}, R_{k,5}\right)\right)\right], \tag{8}$$

which should be maximized to get a parameter estimation of $\theta$. By taking the logarithm and swap the sign, we can formulate a minimization task, which is solved by using a PSO algorithm.

The tracklet duration is limited to a couple of minutes and the purpose is to observe satellites in orbit, thus we assume that the object follows the Keplerian motion model. Theoretically there are many possible parametrizations of a Kepler orbit like classical Keplerian elements $\theta_{g,Kepler} = [a, e, i, \Omega, \omega, \nu]$ or a state vector $\theta_{g,state} = [x, y, z, \dot{x}, \dot{y}, \dot{z}]$ at the time $g$. Since we are using detections with the structure of $[u_k, v_k, \rho_k, \dot{\rho}_k, \ddot{\rho}_k]$ we can create a Mixed Orbital Elements (MOE) parametrization using modified equations from [9]. This parameter set contains the detection and an additional variable, the Semi-Major Axis (SMA) $a$, resulting in $\theta_{g,MOE} = [u, v, \rho, \dot{\rho}, \ddot{\rho}, a]$ at the time $g$. As reference time $g$ we choose the middle epoch of the tracklet. This parameterization has the advantage that we can easily find upper and lower bounds of the search space for the orbit estimation. The upper and lower bounds are passed to the PSO algorithm which tries to minimize the negative log likelihood. After convergence or a maximum number of iterations the PSO provides an estimation of the orbit. This is propagated to all detection times and the ambiguity is resolved analog to the previous method.

We have used the PSO implementation from [4]. In theory there is no guarantee that the PSO converges to the global minimum. In practical studies we have seen that the PSO sometimes converged to a local minimum since we are using randomly placed initial particles inside the search space. To overcome this problem we use a number of $d_{PSO}$ parallel runs and take the result with the lowest cost, hoping that this will give the global minimum. In the following analyses we have set $d_{PSO} = 40$. The number of Gaussians is set to $J = 5$. Another important point is to determine the weights $w_j$. As we will present later in this paper we can see empirically that with increasing SNR the probability of having a wrong ambiguity is reduced. Hence, the weights are set, dependent on the SNR, to the relative frequency at which the respective ambiguity appeared in the analyzed experiments. Overall the method can be summarized as follows:

1. Determine search space $[u, v, \rho, \dot{\rho}, \ddot{\rho}, a]$ based on detection at time $g$
2. Run $d_{PSO}$ parallel PSO
3. Calculate minimum cost of $d_{PSO}$ runs and get the corresponding orbit
4. Propagate the orbit to get the radial velocity and correct the radial velocity measurements

## 4. EXPERIMENTS

This section will present and evaluate five experiments performed with GESTRA: Both a search mode and a tracking mode are presented for Sentinel-3A and Swarm-C, as well as a single tracking mode for Sentinel-3B. All of these satellites have a high SNR of over 40 dB in zenith. Since a high SNR usually means that the correct ambiguity will appear more often, this might not be an appropriate test. Hence, five more artificial experiments were created by adding noise to the aforementioned experiments, such that the resulting tracklet had a maximum SNR between 21 dB and 26 dB, yielding a total of ten experiments. The precise orbit reference data for the Sentinel satellites was downloaded from the Copernicus project website [2], while the Swarm reference data was taken from [3]. In each case, the further analysis was restricted to those detections that are sufficiently close to the object of interest, removing outliers and detections of other objects.

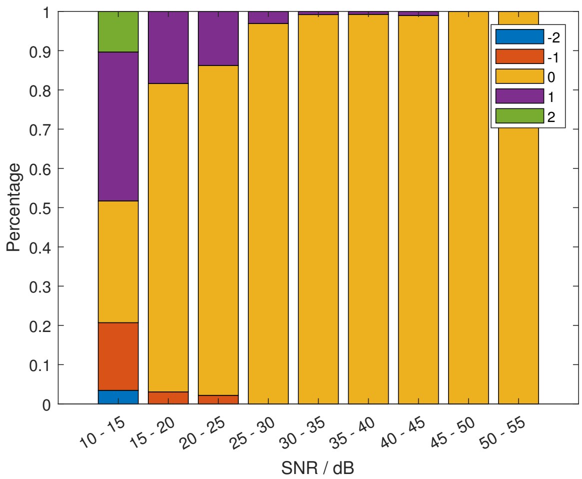


*Figure 3. Percentage of detections in each ambiguity, grouped by SNR. This combines the correlated detections from all ten experiments. The value* 0 *means that the correct ambiguity is found, the value* $+1$ *means that the estimated radial velocity is one ambiguity higher than the reference one etc.*

Figure 3 shows how many detections with a certain SNR lie on which ambiguity. As expected, a high SNR helps to avoid getting the wrong ambiguities, since even the small difference in the local maxima of the ambiguity function will be clearly visible with a sufficiently high SNR. This illustrates that resolving the ambiguities may be more difficult for low SNR targets.

### 4.1. Performance of the methods

Further analysis is about the results of the different methods. All three methods – the RVP, the WLS and the GSF method – were applied to all ten experiments. In addition, they were not only applied to the full tracklet, but starting from the first three detections to the complete tracklet length in steps of two detections. Since a lower detection count impedes ambiguity resolution, this can show the relative performance of the algorithms in a better way.

Figure 4 shows the percentage of incorrectly resolved detections for each of these scenarios. We see that the GSF method clearly shows the best results. The RVP method performs well in most tracking mode experiments, while it fails in the search mode experiments. This is most likely due to the long temporal gaps between the detections: Since there can be more than 5 s between two consecutive detections, the radial motion may not be sufficiently approximated by a quadratic function. Moreover, small errors in the estimation of the radial acceleration can have a large effect – and radial acceleration errors are generally larger in search modes because of the reduced CPI length. In that case, a failure of the RVP method is expected. Here, the WLS method usually outperforms the RVP method. However, especially in the tracking mode experiments without noise, the WLS method needs many detections to achieve correct resolution of all the detections. This is surprising, because in these experiments, the SNR is usually high and hence, most detections will lie on the correct ambiguity already.

There are numerous possible reasons for the rather poor performance of the WLS. One aspect is that the method relies on a Herrick-Gibbs initialization which might lead to large errors for such small angles between the detections due to low time differences. It should be noted that the begin of the tracklets especially during tracking modes is at low elevation and might therefore lead to a reduced SNR and DoA estimation accuracy and consequently less accurate initial states. Since the GSF do not use the Herrick-Gibbs initialization technique but consider the whole search space of the orbit, an improvement would be expected here. Another improvement of performance of the GSF with respect to the WLS should be expected resulting from the aspect of using not only DoA and range, but the full information of the detections, including radial velocity and acceleration.

### 4.2. Self-assessment of the results

The next question is, whether the methods can indicate themselves, how likely it is that their result is correct. The RVP method provides the uncertainty value for this, described in the section 3.1. For the other two methods, we can use the NIS [1], which is supposed to be a good indicator. We determine the residuals between propagation and measurement in all parameter dimensions and utilize the measurement noise variances to get the NIS. Basically, this is small if an orbit is found that fits the data relatively well. If no orbit fits the data, then this is larger. It should be noted that we are using uncertainties based on theoretical assumptions and not empirical ones, which also leads to an increase in this metric if they are too optimistic. Moreover, the number of detections in a tracklet can be an indication, since for a low number of detections, many methods fail. Figure 5 shows the uncertainty/NIS for all methods, indicating whether they were successful – all ambiguities were resolved correctly – or not. We see that the proposed measures work relatively well for the RVP and the WLS method, even though they are not perfect. It might be difficult to be entirely sure that the result is correct, but it is certainly possible to detect the vast majority of failed resolution attempts by filtering out high uncertainty/NIS. For the GSF method, there are not enough such failed attempts in total to allow an assessment whether the NIS is suitable.

### 4.3. Computational costs

Even though a thorough analysis of computing time is beyond the scope of this work, we will give a brief picture of the computational costs required. The times noted here are the computation times on a notebook workstation for resolution of a single tracklet. Because of its simplic-

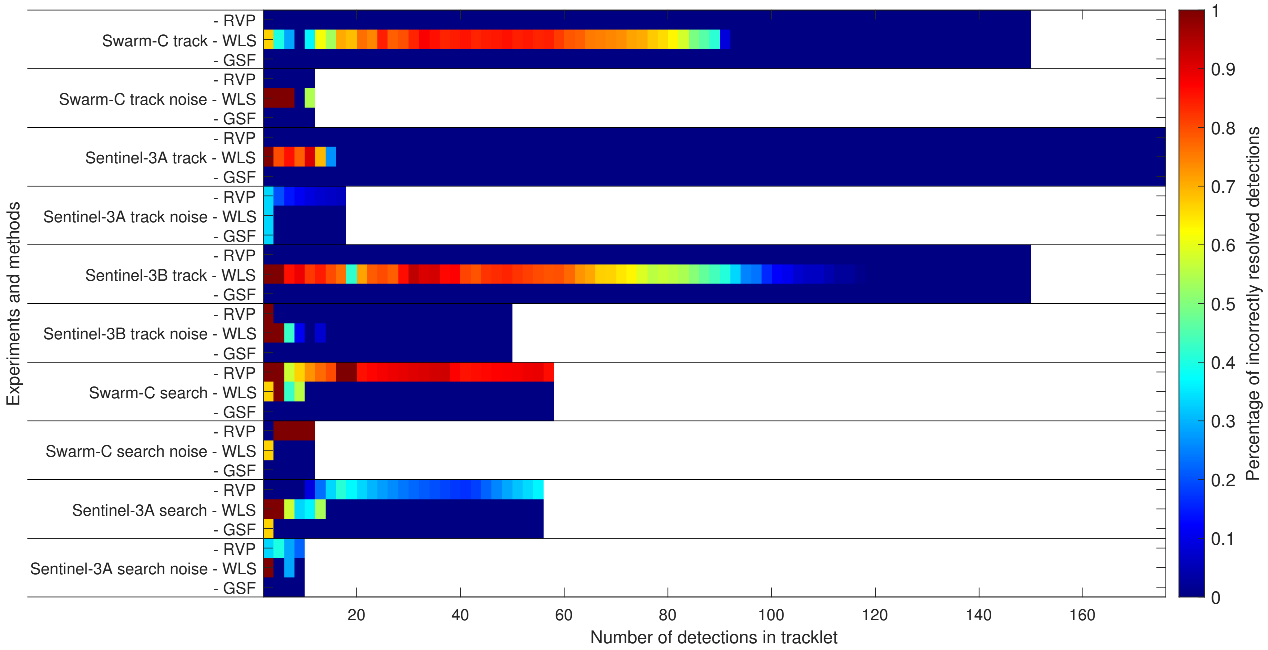


*Figure 4. Percentage of incorrectly resolved detections by method by experiment. White means that the experiment did not have as many detections.*

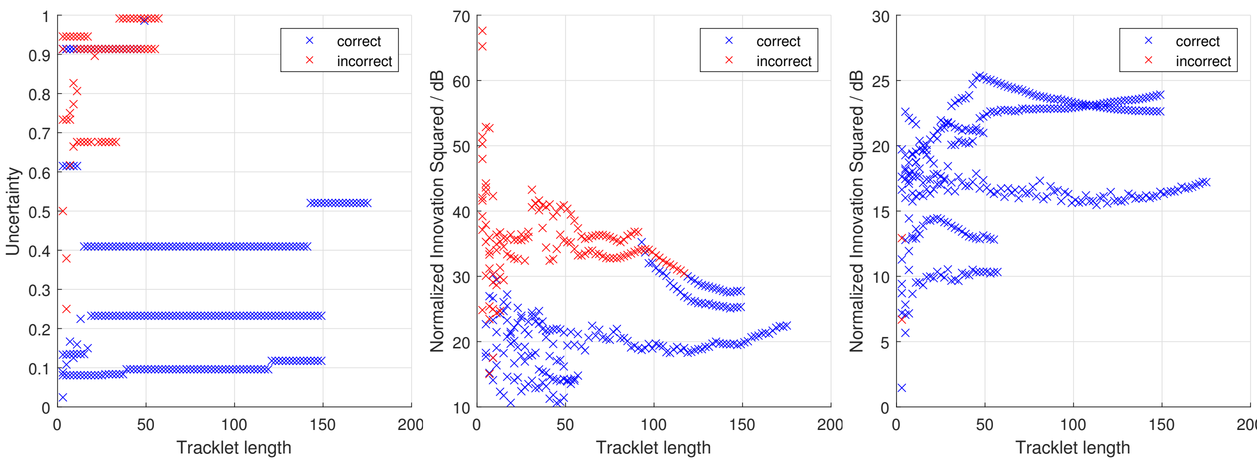


*Figure 5. The methods' confidence in the results. These plots combine all ten experiments and all tracklet lengths. Left: RVP method, $y$ axis shows uncertainty defined in section 3.1. Middle: WLS method, $y$ axis shows NIS. Right: GSF method, $y$ axis also shows NIS.*

ity, the RVP method is by far the fastest, as no optimization or orbit determination is required. In the tests presented here, all examples took less than $0.2\,\mathrm{s}$. It should be noted that this was the only method implemented in C++, while the other methods were implemented in MATLAB, which might also have contributed to high difference in computational cost. The WLS method was considerably slower, maximum runtimes were about $10\,\mathrm{s}$. However, by far the slowest method was the GSF method because of two reasons: On the one hand the PSO algorithm is slower than the WLS, because it needs more iterations for convergence. On the other hand, the need for multiple attempts in the GSF method to prevent convergence to local minima increases the runtime. The maximum runtime of this method was about $20\,\mathrm{min}$. Hence, the realization of the GSF method on a real-time radar system would require some form of speed-up, either through more efficient code or parallelization.

## 5. CONCLUSION

In this work, we have investigated three methods to resolve Doppler ambiguities in pulsed radar systems, among which two were introduced here. They show different complexities and have shown their performance using data from the GESTRA system. The second method developed here using a GSF in combination with a PSO to do IOD performed best in the analyzed experiments. Among the others, RVP is usually better in tracking modes, while WLS is superior in search modes.

An essential next step is to implement the proposed concepts on the radar system and analyze a larger amount of experiments. Besides, there is room for improvement in the GSF method. Tuning the parameters of the PSO or even change the numerical optimization algorithm to one which is more stable in terms of finding the global optimum for this kind of likelihood functions. With the upcoming extension of the GESTRA system with a second receiver, the proposed methods need to be extended to a multistatic radar network.

## ACKNOWLEDGMENTS

The authors would like to thank Erik Busley and Ludger Prünte for proofreading the manuscript. Moreover, the authors would like to thank the development team of GESTRA, consisting of more than 70 members, for their work. The development of the GESTRA system was performed on behalf of the German Space Agency with funds of the German Federal Ministry for Economic Affairs and Climate Action (BMWK) under the contract No. 50LZ1401.

In a few sections, FHGenie, an instance of ChatGPT hosted by the Fraunhofer Gesellschaft, was utilized to improve the language style.

## REFERENCES

1. Yaakov Bar-Shalom, X. Rong Li, and Thiagalingam Kirubarajan. *Estimation with applications to Tracking and Navigation*. John Wiley & Sons, Inc., 2001.
2. ESA. Copernicus Sentinel Orbit data. `https://dataspace.copernicus.eu/`, 2024. [Online; accessed July 25, 2024].
3. ESA. Swarm Data Access. `https://swarm-diss.eo.esa.int/`, 2024. [Online; accessed January 07, 2025].
4. Matthew Kelly. Particle Swarm Optimization. `https://de.mathworks.com/matlabcentral/fileexchange/54849-particle-swarm-optimization`, 2024. [Online; accessed October 22, 2024].
5. Donald J. Kessler and Burton G. Cour-Palais. Collision frequency of artificial satellites: The creation of a debris belt. *Journal of Geophysical Research: Space Physics*, 83(A6):2637–2646, 1978.
6. Nadav Neuberger. *Signal Processing for Space Surveillance Radar*. PhD thesis, Siegen University, 2022.
7. Nadav Neuberger, Simon Kollecker, Martin Käske, Steven Horstmann, and Ludger Prünte. GESTRA: First Results of LEO Object Parameter Estimation. In *2nd NEO and Debris Detection Conference*, 2023.
8. ESA Space Debris Office. ESA's Annual Space Environment Report. `https://www.sdo.esoc.esa.int/environment_report/Space_Environment_Report_latest.pdf`, 2024. [Online; accessed March 18, 2025].
9. Jinye Qu, Defeng Chen, Huawei Cao, Tuo Fu, and Shuo Zhang. Initial Orbit Determination Method for Low Earth arbit Objects Using Too-Short Arc Based on Bistatic Radar. *IEEE Access*, 10:76766–76779, 2022.
10. Isabel Schlangen and Martin Käske. Resolving Multimodal Angular Measurements in Coherent Radar Networks using Bayesian Estimation. In *Proceedings of the 9th European Conference on Space Debris*, 2025. [Submitted and accepted].
11. Sang-Jin Shin and Eun Hee Kim. Track-Before-Resolving: Doppler ambiguity resolution at low SNR. *IET Radar Sonar and Navigation*, 17(1):117–127, 2023.
12. Merrill I. Skolnik. *Radar Handbook, Third Edition*. Electronics electrical engineering. McGraw-Hill Education, 2008.
13. Xiping Sun, Xipeng Wu, Qinquan Zhou, Lei Zhang, and Jianxin Wu. Airborne Radar Staggered PRF Coherent Processing Method for Down-Looking Target Detection. *Remote Sensing*, 15(13), 2023.
14. S. A. K. Syed Mohamed, Tworit Dash, Oleg A. Krasnov, Jelle Bout, Rob Van Der Meer, and Alexander G. Yarovoy. Application of Non-Uniform Sampling to Avoid Aliasing in the Precipitation Doppler Spectrum. In *2024 International Radar Symposium, IRS 2024*, Proceedings International Radar Symposium, pages 216–221. IEEE, 2024. Available: [Online].
15. David A. Vallado. *Fundamentals of Astrodynamics and Applications*. Microcosm Press, 4th edition, 2013.
16. Helmut Wilden, Nadya Ben Bekhti, Rudolf Hoffmann, Claus Kirchner, Robert Kohlleppel, Christoph Reising, Andreas Brenner, and Thomas Eversberg. GESTRA – Recent Progress, Mode Design and Signal Processing. In *2019 IEEE International Symposium on Phased Array System Technology (PAST)*, pages 1–8, 2019.
17. Helmut Wilden, Claus Kirchner, Olaf Peters, Nadya Ben Bekhti, Robert Kohlleppel, Andreas Brenner, and Thomas Eversberg. GESTRA – Technology Aspects and Mode Design for Space Surveillance and Tracking. In *Proceedings of the 7th European Conference on Space Debris*, 2017.
18. Zhihua Yuan, Defeng Chen, Shan Xue, and Tuo fu. Solving Velocity Ambiguity for Pulse Doppler Radar Space Target Measurement. *IOP Conference Series: Materials Science and Engineering*, 608:012038, 2019.

19. Gongjian Zhou, Michel Pelletier, Thia Kirubarajan, and Taifan Quan. A Gaussian Mixture filter for target tracking with Doppler ambiguity. *Proceedings of SPIE - The International Society for Optical Engineering*, 8392, 2012.